

VERIFICATION AND VALIDATION OF OPEN WATER TEST OF B4-65 B-SERIES PROPELLER MODEL

Andik Machfudin^{1,2}, A.A.B. Dinariyana^{2*}, Dian Purnama Sari¹

¹ National Research and Innovation Agency, Indonesia

² Marine Engineering Department, Institut Teknologi Sepuluh Nopember, Surabaya, Indonesia

* dinariyana@yahoo.com

Verification and validation (V&V) are essential processes in computational simulations that aim to evaluate the accuracy and reliability of the results compared to experimental data. The quantification of error and uncertainty estimates is crucial in V&V. In this particular study, the open water test of a four-bladed B-series propeller model at 1/6.98 scale was conducted for three advanced coefficients ($J = 0.50$, $J = 0.60$, and $J = 0.70$) at the Indonesian Hydrodynamic Laboratory (IHL). The simulation was conducted under experimental conditions using FINE/Marine 7.2. Verification was performed to estimate the error δ_{REG}^* and the numerical uncertainty U_{SN} according to the ITTC convergence ratio R and order of accuracy P_G . The average uncertainty estimated for the thrust and torque coefficient was found to be between 1.72% to 4.81%, with a 95% confidence level. Reducing errors and uncertainties associated with verification and validation in open-water experiments can increase the reliability of numerical simulations.

Keywords: open water, thrust and torque coefficient, uncertainty, verification, validation

1 INTRODUCTION

Verification and validation (V&V) are critical procedures for evaluating the accuracy and reliability of computational simulations. The verification process involves identifying and quantifying errors in the computational model and its solution, while validation assesses how well the computational results align with experimental data, including the quantification of error and uncertainty for both. Understanding the associated uncertainty is essential for meaningful simulation results. This paper presents a general overview of the V&V approach used in ship hydrodynamics, including methodology and procedures [1]. Several studies have investigated V&V performance in single and twin-propeller performance [2], the trim effect and flow field around the propeller on the propulsion of a free-running ship [3], cavitation behavior of ship propellers [4], cavitating flow around propellers to predict the effects of vorticity generation and cavitation phenomena [5], dynamic loads of propeller open water in regular waves at various submergence depths using the ITTC method [6], and integrating modeling and experimental studies to show effectiveness in practical marine and hydrodynamic applications [7][8].

The B-series propellers as research objects are widely used in numerical simulations. In this study, an adapted numerical simulation of the B-series propeller was performed by the researchers to evaluate the propeller characteristics quantified by thrust, torque, and efficiency coefficients [9]. The researchers also predicted open-water B-series propeller performance from the transformation of the propeller rotation and blade numbers [10] and measured 5-blade B-series propeller noise based on the ITTC Method [11]. The numerical investigation was studied to research the influence of the skew propeller angles and the tension for verification of the prediction cavity and noise cavitation performance [12]. Meanwhile, the probers verified the influence of twin B-Series Propeller in tandem under various designs and loading configurations against performance in open water [13] and particularized angle of skew, which has a thrust value, torque, and high performance with a reduced cavitation risk at the angle 0° [14]. Research of B-series performance is investigated for analyzing engine propeller matching [15] and determining the best propeller for fishing boat activities [16].

The grid type and mesh density greatly affected the precision of the findings, tolerance value, and the unpredictability factor of simulation is the grid type and mesh density. The numerical simulation under an efficient meshing approach of point vorticity cavitation has been researched [17]. In addition, the chosen grid type, mesh density, and turbulence models were inspected to generate a better result of numerical simulation [18]. The FINE / TURBO application was very suitable and facilitated simulation activities for numerical research from propeller open water. The Fine/ Turbo application was applied to investigate the effect of the propeller on the hull while maintaining a low computational effort [19]. Furthermore, the fine/turbo application also was used to investigate the position of the shaft to produce the thrust in the design of high-performance and commercial ships [20]. Further, the investigators presented an increase in the Reynolds number along with the increase in the centrifugal force and the rotating velocity, causing an increase in the cross-flow effect [21]. Also, it was analyzed experimentally how waves and propeller immersion depth affected the open-water propeller [22]. A numerical simulation was conducted to predict benchmark propeller performance in model and full-scale simulations [23] and it investigated blade rotor performance in gravitational vortex turbines [24]. Meanwhile, simulations were conducted to determine the efficiency and optimization of the propeller performance [25][26].

In prior research, a systematic approach was utilized to investigate uncertainty in propeller open-water performance [27]. Experimental investigations with uncertainty analysis were arranged to discover the optimal results [28][29].

According to particular research, the propeller's pitch angle, time, and spatial discretization contributed to total uncertainty [30][31][32]. This involved conducting 5 series of tests with three-speed measurements in each series and identifying 3 advance coefficients (J) and open water propeller characteristic parameters using propeller geometry, rotation rate, and water velocity. The Indonesian Hydrodynamic Laboratory (IHL), as a scientific facility and member of the ITTC, has scrutinized resistance test uncertainty to ensure high accuracy and low failure rates in experiments [33][34][35]. In the present study, CFD verification and validation (V&V) were performed on the time-averaged thrust and torque (K_T and K_Q) of a propeller model according to ITTC standard methodology. The study also includes a comparison of experimental and simulated K_T and K_Q values. An open water test was conducted on a bronze propeller model at IHL, and simulation was performed using the FINE/Marine 7.2 ISIS-CFD program.

2 EXPERIMENTAL PROCEDURE

The focal point of the investigation was the B-Series propeller model, which was subjected to experimentation in a towing tank located at the Indonesian Hydrodynamic Laboratory. The propeller model in question was a conventional one that underwent routine testing at the laboratory. To conduct the propeller dimension, a precision automatic milling machine was employed to manufacture the propeller, which was executed with a high level of accuracy. The relevant parameters are detailed in Table 1, while the propeller's geometry is depicted in Figure 1. The model was constructed on a 1/6.98 scale. The towing tank used for open-water observations was of substantial dimensions, measuring 234.5 m (including the harbor), 11 m, and 5.5 m in length, width, and depth, respectively. The carriage's maximum speed in the towing tank was 9 m/s. The open water dynamometer H-39 was utilized to conduct the tests, which was developed and designed by Kempf & Remmers.

Table 1. Main particulars of the research object

Parameter	Value
Propeller types	B-Series
Number of blades (Z)	4
Diameter (D)	157.6 mm
Propeller Pitch ratio (P/D)	1.133
Pitch 0.7 R	178.6 mm
Blade Area Ratio (A_E/A_0)	0.65
Rotation	Right Hand

where P is pitch, A_E refers to propeller expanded area, A_0 refers to propeller disk area, D represents diameter of the propeller, and Z refers to number of blades. At table 2, J represents advance coefficient, K_T represents thrust coefficient, and K_Q refers to torque coefficient.

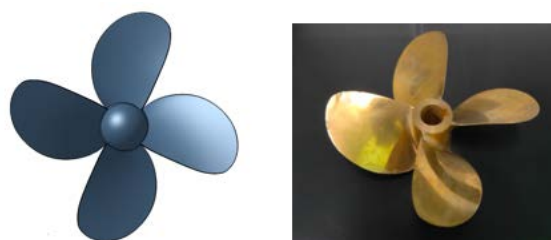


Figure 1. The geometry of the propeller

This study employed five sets of tests, each containing three velocity measurements, to investigate the uncertainty of open water conditions. The total number of test points was 15, as presented in Table 2. To measure the performance, three advance coefficients ($J = 0.50$, $J = 0.60$, and $J = 0.70$) were utilized. The towing force, which was measured in kilograms, was converted to Newtons (N) by multiplying it with the acceleration due to gravity, $g = 9.8$ m/s. Consistent with the International Towing Tank Conference (ITTC) recommendation, water temperature was observed at each run using a digital thermometer.

Table 2. The thrust and torque coefficients data tests

Run/ Test	J = 0.50		J = 0.60		J = 0.70	
	K_T	K_Q	K_T	K_Q	K_T	K_Q
1	0.32693	0.06214	0.27110	0.05327	0.23411	0.04942
2	0.31557	0.05721	0.27472	0.05386	0.22510	0.04880
3	0.31605	0.05878	0.28202	0.05537	0.22212	0.04835
4	0.32148	0.05975	0.26690	0.05233	0.22078	0.04471
5	0.31377	0.05991	0.27179	0.05211	0.22645	0.04781
6	0.31472	0.06118	0.27424	0.05193	0.22453	0.04505
7	0.31012	0.05975	0.27238	0.05193	0.22436	0.04901
8	0.31280	0.06063	0.27499	0.05319	0.22931	0.04908
9	0.31082	0.06008	0.27203	0.05284	0.22931	0.05035
10	0.31507	0.06132	0.27338	0.05414	0.22579	0.04857
11	0.31097	0.05862	0.27040	0.05266	0.22831	0.04913
12	0.31296	0.05927	0.27131	0.05259	0.22795	0.05036
13	0.31526	0.06020	0.27306	0.05371	0.22582	0.04883
14	0.31645	0.06429	0.26808	0.05422	0.22905	0.04911
15	0.32513	0.06175	0.26395	0.05384	0.22342	0.04826
Mean	0.31587	0.06033	0.27202	0.05320	0.22643	0.04846

3 NUMERICAL METHOD

A B-Series propeller model was presented in right-handed rotation at three speeds, 1.735, 2.082, and 2.429 m/s (corresponding to a variation from $J = 0.50$, $J = 0.60$, and $J = 0.70$ in the advance coefficient). Using the FINE/ Marine 7.2 ISIS-CFD program, the incompressible Reynolds-averaged Navier Stokes (RANS) equations were solved, and the thrust and torque of open water were estimated. The space-time calculation of finite volumes was used by the solver. Modeling the free surface was done using an interface-capturing strategy.

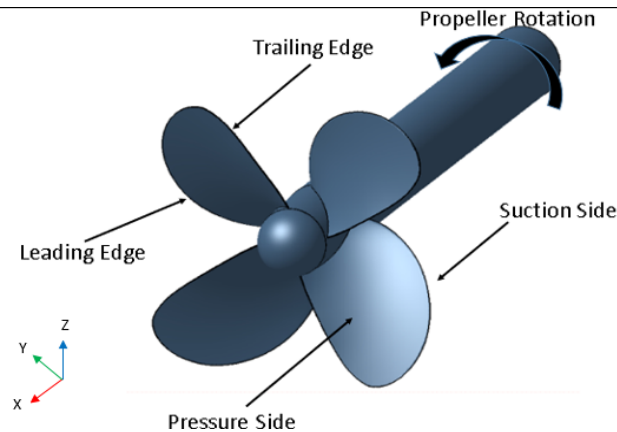


Figure 2. The propeller's geometry characteristics

The simulations employed imported geometrical measurements for meshing, solution, and postprocessing. The initial steps in the modeling were creating mesh generation and computational setup. A geometry setup was performed to develop an acceptable mesh for simulation. Meanwhile, to give the propeller more flexibility with variable mesh levels of refinement, the propeller was divided into several patches: the shaft, hub, cap, blade coarse mesh, Blade fine mesh, Tip, and Fillet. The blade tip had a significant level of curvature at the leading and trailing edges; consequently, a more detailed geometry was necessitated to represent the characteristics, as seen in Figure 2.

The performance parameters of the propeller showed how it behaved under a constant load and uniform flow. The parameters of the open water test were presented as propeller thrust and torque, K_T and K_Q , compared to the advance coefficient, J , and efficiency, η . The parameters are described as follows:

$$J = \frac{V_a}{nD} \quad (1)$$

$$K_T = \frac{T}{\rho n^2 D^4} \quad (2)$$

$$K_Q = \frac{Q}{\rho n^2 D^5} \quad (3)$$

$$\eta = \frac{J K_T}{2\pi K_Q} \quad (4)$$

where ρ is the water density, n refers to the rotational speed in revolutions per second (rev/sec), D represents the diameter of the propeller in meters, T refers to the thrust, Q represents the torque and V_a refers to fluid velocity in meters per second (m/s).

By adjusting the fluid's density and viscosity, the model's fluid properties were simulated. The water had a density of 996.5 kg/m^3 and a dynamic viscosity of $1.04362 \cdot 10^{-3} \text{ Pa}\cdot\text{s}$. The general parameters of the numerical control involved saving the result after every 50 iterations while executing calculations for 1000 iterations with second-order convergence criteria and five nonlinear iterations.

As a component of a verification analysis aimed at determining the optimal grid spacing for simulation models, the numerical uncertainties were assessed. The accuracy order of the results was evaluated through implementation of the grid convergence index (GCI) methodology, which was built upon Richardson extrapolation. In compliance with the ITTC's guidelines, uncertainty analysis was conducted using solutions produced by RANS equations. To measure the grid errors and uncertainties, three different grids were examined, namely, grids 1-2 and grids 2-3. It is mandatory to carry out at least three solution analyses for the purpose of convergence investigations. To assess the sensitivity and convergence, more than two solutions were required. The convergence ratio is described as the distinction between the medium-fine $\varepsilon_{21} = S_2 - S_1$ and coarse medium $\varepsilon_{32} = S_3 - S_2$ solutions:

$$R_G = \frac{\varepsilon_{21}}{\varepsilon_{32}} \quad (5)$$

Three convergence conditions are identified according to the grade of R_G as follows:

1. Monotonic Convergence: $0 < R_G < 1$
2. Oscillatory Convergence: $R_G < 0$
3. Divergence: $R_G > 1$

Stern's verification processes state that several solutions should be used when using iterative and parametric convergence investigations in at least three conditions. While keeping the constant grades of another parameter, this study was also carried out utilizing systematic parameters. A uniform refinement ratio can be studied, as shown below:

$$r_G = \frac{\Delta x_2}{\Delta x_1} = \frac{\Delta x_3}{\Delta x_2} \quad (7)$$

Δ_x show the initial mesh ratio, Δ_{x_3} refers to fine, Δ_{x_2} refers to medium, and Δ_{x_1} represents coarse. The refinement ratio can be acceptable if it has a value of $\sqrt{2}$ [36]. Roache's research suggests that $r_G = 2$ might be too large for commercial CFD simulations. In the verification and validation investigations for this research, non-cavitating conditions were used with $r_G = \sqrt{2}$ for the grid.

The three solutions in Richardson extrapolation (RE)-based techniques were utilized to generate estimations for inaccuracy and order of accuracy:

$$\delta_{REG}^* = \frac{\varepsilon_{G,21}}{r_G^{P_G-1}} \quad (8)$$

$$P_G = \frac{\ln(\varepsilon_{G,32}/\varepsilon_{G,21})}{\ln(r_G)} \quad (9)$$

The grid level of the fine mesh was calculated using a factor of safety (F_S) technique [35], where an error estimate from RE was multiplied by an F_S to constrain simulation errors as follows:

$$U_G = (F_S - 1) |\delta_{REG}^*| \quad (10)$$

The grid uncertainty U_G and the numerical uncertainty U_{SN} were equivalents [1]. The difference in error (E) between the CFD and the EFD was contrasted to the validation of uncertainty to see if the simulation had been validated, which would be generated as:

$$U_V^2 = U_D^2 + U_{SN}^2 \quad (11)$$

The equation can be applied to calculate the error (E) between simulation and experiment results:

$$E = D - S \quad (12)$$

Where D represents the resulting value by the experiment, and S represents the value attained through simulation. This validation method states that the simulation is verified at the U_v level if $|E| < U_v$. If $(U_v < |E|)$ instead, it is possible to make improvements using the sign and magnitude of E [1].

4 RESULTS AND DISCUSSION

Different initial meshes result in various mesh sizes, enabling the refining of the whole fluid volume rather than just the regions close to the solid components. Figures 3 and 4 describe the fully created coarse, medium, and fine meshes, which range in size from 1.3 to 6.0 million cells, and advance coefficient of $J = 0.50$, $J 0.60$, and $J 0.70$. According to the Figures, the tip section, leading edge, and trailing edge of the propeller all have the highest mesh node densities.

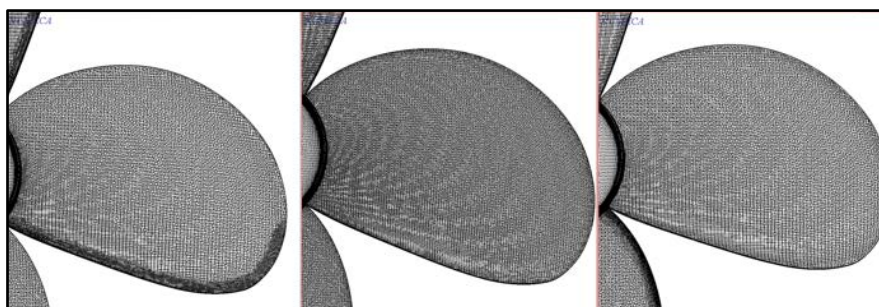


Figure 3. The generated mesh of the propeller blade (course, medium, and fine grid)

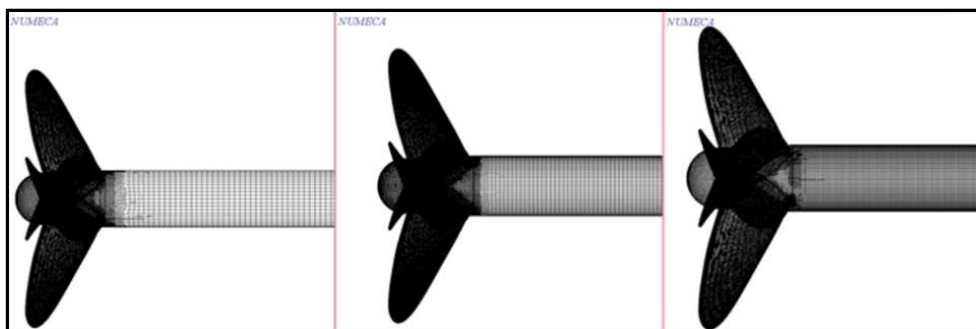


Figure 4. The generated mesh of propeller hub (course, medium, and fine grid)

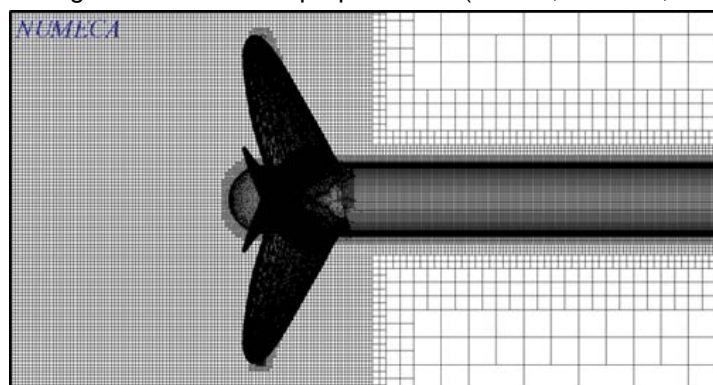


Figure 5. Mesh around the surface (fine grid)

Regarding the initial mesh size, all improvements were implemented. The created fine mesh that encircles the surface location is presented in Figure 5. According to the internal surface's form, more mesh refinement was applied. The stability and calculation outcome were unaffected by the grids' high quality, which was provided in all constructed grids. Maintaining decent mesh quality was critical for reducing discretization errors. Measures of mesh orthogonality, expansion ratio, and aspect ratio (or stretching) are three categories of essential mesh quality indicators.

Figures 6 and 7 represent the contour plots of the hydrodynamic pressure impacting the propeller surface at fine mesh. Pressure levels were indicated by the colors on the propeller surface. The highest pressure occurred at tip of the propeller blade, while the lowest pressure mainly occurred on the inner part of the blade, either in the trailing or the suction side area. The highest pressure was found on the blade's edge, as presented in the red part of the image, while the lowest pressure was observed on the propeller's suction side, as seen in the blue portion of the same image.

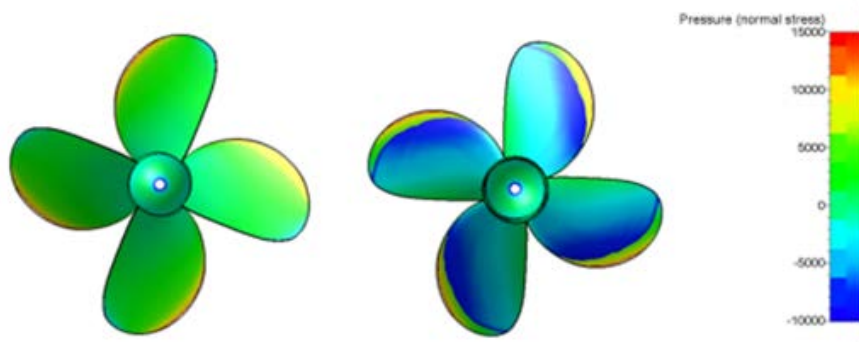


Fig. 6. Hydrodynamic Pressure in the pressure side (left) and suction side (right) in a fine grid

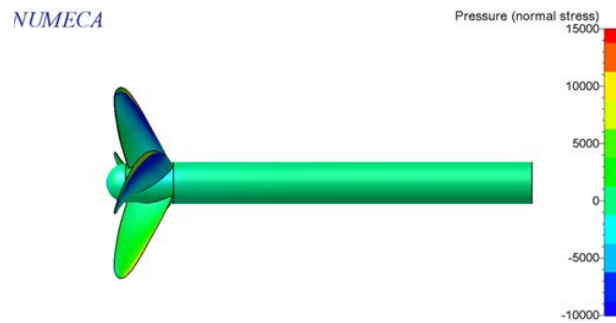


Fig. 7. Hydrodynamic Pressure in the hub (fine grid)

Velocity parameters of the open water propeller modeling are shown in Figure 8. At the propeller blade's tip, where the speed was maximum, an increase in the fluid's flow velocity contributed to the highest fluid velocity in that area. The images in the yellow portion of the diagram represented the area of the maximum fluid velocity on the blade. In contrast, the image in the blue section represented the spot of the lowest fluid velocity on the back of the propeller. The route of the value with a negative sign is the inverse of the route of the entering fluid flow.

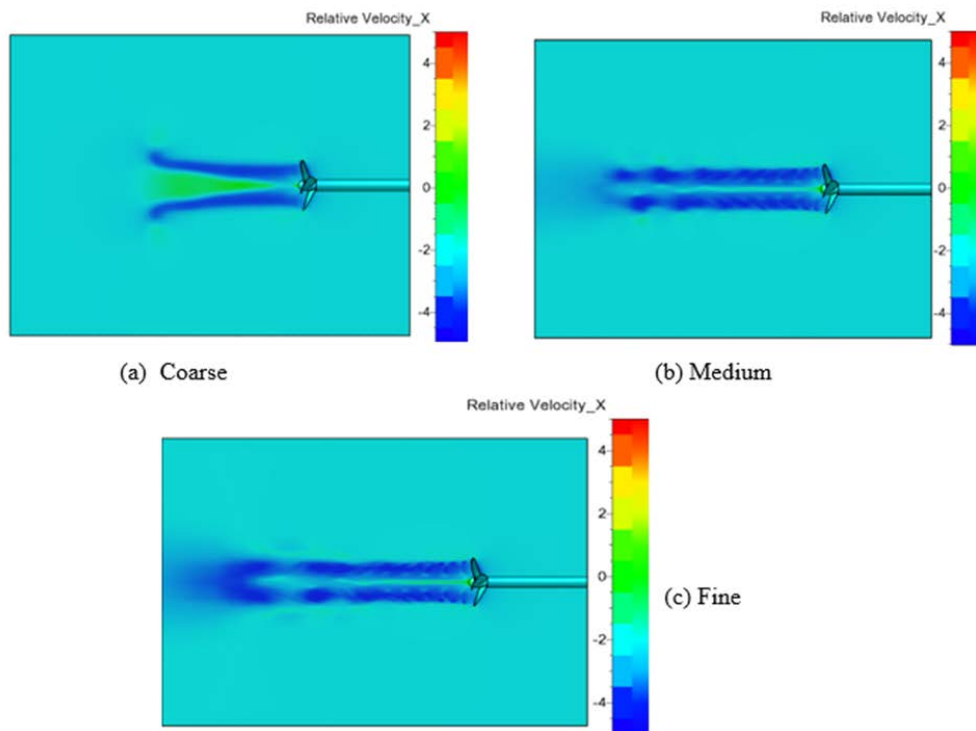


Figure 8. The velocity of the simulation. a) coarse, b) medium, c) fine

Results of mesh convergence study at advance coefficients J of 0.50, J 0.60, and J 0.70 are shown in Table 3-5. Figure 9 describes the thrust coefficient (K_T) of the propeller model, torque coefficient (K_Q), and efficiency (η) of the experimental data (EFD) and model grid variability of simulation (CFD) at $J=0.60$. Further, a comparison of experimental data and the result of the simulation, showed the thrust coefficient (K_T) for fine-grid convergence data is almost similar to the experimental data, and the result of the fine mesh has higher efficiency than another mesh in

the simulation. It indicates that the solution converged on a value as the mesh size was increased. Consequently, subsequent calculations in this situation should be performed using fine mesh.

Table 3. Comparison of mesh convergence study at $J=0.50$.

Characteristics	Mesh density			ϵ_{21} [%]	ϵ_{32} [%]
	Coarse grids	medium grids	fine grids		
KT	0.3236	0.3217	0.3206	0.34%	0.93%
KQ	0.0587	0.0576	0.0573	0.52%	1.97%
η	0.4389	0.4447	0.4455	0.18%	1.29%

Table 4. Comparison of mesh convergence study at $J=0.60$

Characteristics	Mesh density			ϵ_{21} [%]	ϵ_{32} [%]
	Coarse grids	medium grids	fine grids		
KT	0.2808	0.2760	0,2753	0.25%	1.71%
KQ	0.0523	0.0510	0,0508	0.39%	2.49%
η	0.5130	0.5170	0,5178	0.14%	0.79%

Table 5. Comparison of mesh convergence study at $J=0.70$

Characteristics	Mesh density			ϵ_{21} [%]	ϵ_{32} [%]
	Coarse grids	Medium grids	fine grids		
KT	0.2321	0.2292	0.2287	0.22%	1.25%
KQ	0.0475	0.0467	0.0465	0.43%	1.68%
η	0.5447	0.5471	0.5482	0.21%	0.44%

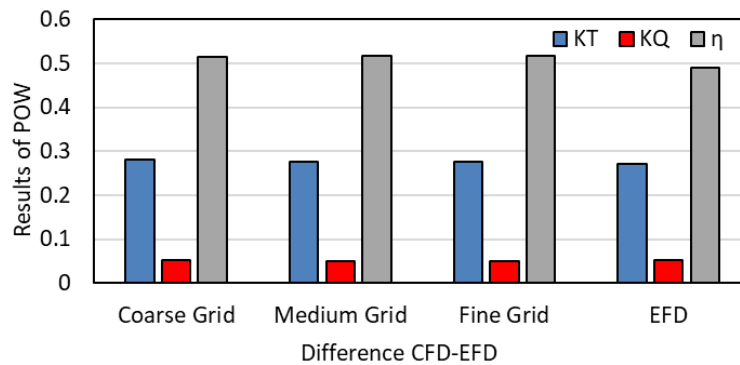


Figure 9. Simulation and experimental for open water calculation at $J=0.60$

Tables 6 and 7 represent validation and Verification results for Thrust Coefficient (K_T) and Torque Coefficient (K_Q). They describe three grids of convergence ratio (R_G), and generalized Richardson Extrapolation (RE) was used to estimate the error (δ_{RE}^*) and order of accuracy (P_G). An error was multiplied by a factor of safety (FS) to define simulation numerical uncertainty (U_{SN}) and comparison error (E). The uncertainty of the simulation measurement was then validated using experimental data of the open water uncertainty in the IHL Towing Tank, as presented in the previous study.

Table 6. Verification data for Thrust Coefficient (K_T) on hydrodynamic performance

J	ϵ_{32}	ϵ_{21}	R_G	P_G	U_G	U_D	U_V	E
0.5	-0.00190	-0.00110	0.57894	1.57767	-0.00037	0.01720	0.01720	-0.00470
0.6	-0.00480	-0.00070	0.14583	5.55763	-0.00003	0.01981	0.02151	-0.00330

J	\mathcal{E}_{32}	\mathcal{E}_{21}	R_G	P_G	U_G	U_D	U_V	E
0.7	-0.00290	-0.00050	0.17241	5.07431	-0.00003	0.02362	0.02362	-0.00230

Table 7. Verification data for Torque Coefficient (K_Q) on hydrodynamic performance

J	\mathcal{E}_{32}	\mathcal{E}_{21}	R_G	P_G	U_G	U_D	U_V	E
0.5	-0.00112	-0.00010	0.04464	8.97476	-5.84E-07	0.03875	0.03879	0.00274
0.6	-0.00132	-0.00020	0.00757	14.09493	-1.91E-08	0.04346	0.04347	0.00228
0.7	-0.00089	-0.00020	0.02247	10.95624	-1.15E-07	0.04812	0.04812	0.00435

The objective of validation is to evaluate the level of modeling uncertainty, which pertains to the degree to which the mathematical model accurately reflects the physical reality. The disparity between the simulation and experimental data is referred to as the comparison error (E), which can be compared to the total validation uncertainty (U_V). The latter encompasses not only numerical uncertainties but also experimental uncertainties. The final outcomes may be validated within the bounds of uncertainty if both the comparison error (E) and validation uncertainty (U_V) are relatively low. In cases where the comparison error exceeds the validation uncertainty, it is likely that the modeling error predominates the comparison error, signifying the need for model refinement. In the current investigation, the comparison error results (E) are inferior to the validation uncertainty results (U_V), denoting that the outcomes are validated within the bounds of uncertainty. There was a sufficient agreement between the experimental and simulation data for open water. According to the application of eq.(5)-(11) in the calculations obtained from tables 6 and 7, the validation uncertainty values of the thrust coefficient were at 1.72% to 2.36% and 3.87% to 4.81% for the validation uncertainty values of the torque coefficient. Based on the research conducted, the numerical model was dependable and coherent. The threshold value of uncertainty was still required, which was below 5%.

5 CONCLUSIONS

Various research methodologies necessitate the integration of uncertainty analysis as a validation technique to ensure coherence and reliability. Verification and validation (V&V) are the principal means of assessing the accuracy and dependability of numerical outcomes, encompassing quantified measures of error and uncertainty. Through the identification of an appropriate grid resolution for simulations, a verification investigation was conducted to appraise numerical uncertainty. Using the FINE/ Marine 7.2, the simulation was performed following the experimental conditions at three different speeds (advance coefficient $J = 0.5, 0.6,$ and 0.7). Verification determined three grids of convergence ratio (R_G), and generalized Richardson Extrapolation (RE) was used to estimate the error ($\delta_{RE_G}^*$) and order of accuracy (P_G). An error was multiplied by a factor of safety (FS) to define simulation numerical uncertainty (U_{SN}). The research was conducted by comparing error results and validation uncertainty results. It represents the results were validated with uncertainty. The validation uncertainty of the thrust coefficient was described at 1.72% to 2.36% and 3.87% to 4.81% for the validation uncertainty of the torque coefficient. The research findings demonstrated the dependability and coherence of the modeling and experimental, and the acceptable threshold for uncertainty is 95% of the confidence level. Considering this research's findings, further study is necessary to investigate the uncertainty analysis of propulsion tests in the hydrodynamic laboratory.

6 ACKNOWLEDGEMENT

The present study was underpinned by The National Research and Innovation Agency (BRIN) which has provided funding for research-based educational programs, under the grant number SP/112/BPPT/08/2021. The BRIN's commitment to research has been instrumental in enabling the authors to conduct this investigation and disseminate the findings to the scientific community. The authors would like to acknowledge the valuable assistance and support received from the staff members of The Indonesian Hydrodynamic Laboratory, which has significantly contributed to the successful completion of the experiment.

7 REFERENCES

- [1] Stern, F., Wilson, R. V., Coleman, H. W., Paterson, E. G. (2001). Comprehensive approach to verification and validation of CFD simulations—Part 1: Methodology and Procedures. *Journal of Fluids Engineering*, vol. 123, 2001, 793-802, DOI: 10.1115/1.1412235.
- [2] Lungu, A. (2021). Numerical assessment of twin-propeller performances. *IOP Conference Series: Earth and Environmental Science* 2021, p. 012022.
- [3] Wang, J., Wan, D., Maksoud, M. A. (2020). CFD investigations of ship propulsion performance at different trim angles. *International Ocean and Polar Engineering Conference* 2020, vol. 30.
- [4] Nouroozi, H., Zeraatgar, H. (2019). A reliable simulation for hydrodynamic performance prediction of surface-piercing propellers using URANS method. *Applied Ocean Research*, vol. 92, 2019, 101939, DOI :10.1016/j.apor.2019.101939,

- [5] Long, Y., Han, C., Ji, B., Long, X., Wang, Y. (2020). Verification and validation of large eddy simulations of the turbulent cavitating flow around two marine propellers with emphasis on the skew angle effects. *Applied Ocean Research*, vol. 101, January 2020, 102167, DOI: 10.1016/j.apor.2020.102167.
- [6] Zhang, W., Ma, N., Gu, X., Feng, P. (2021). RANS simulation of open propeller dynamic loads in regular head waves considering coupled oblique-flow and free-surface effect. *Ocean Engineering*, vol. 234, 2021, 108741, DOI: 10.1016/j.oceaneng.2021.108741.
- [7] Hussein, K. B., Ibrahim, M. (2022). Experimental and numerical study on the hydrodynamic performance of suspended curved breakwaters. *Nase More*, vol. 69, no. 3, 411121.
- [8] Piskur, P., Szymak, P., Flis, L., Sznajder, J. (2020). Analysis of a fin drag force in a biomimetic underwater vehicle. *Nase More*, vol. 67, no. 3, 192-198, DOI:10.17818/NM/2020/3.2.
- [9] AmiraAdam, N., Fitriadhy, A., Quah, C., Haryanto, T., and Koto, J., "Prediction of propeller performance using Computational Fluid Dynamics (CFD) approach," *Proceeding Martec, 11th International Conference on Marine Technology*, 2018, https://www.mtc-utm.my/wp-content/uploads/MARTEC_2018_Paper/N1.pdf.
- [10] Amira, A. N., Fitriadhy, A., Quah, C. J., Haryanto, T. (2020). Computational analysis on B-series propeller performance in open water. *Marine Systems & Ocean Technology*, vol. 15, 2020, 299–307, DOI: 10.1007/s40868-020-00087-z.
- [11] Ebrahimi, A., Razaghian, A. H., Tootian, A., Seif, M. S. (2021). An experimental investigation of hydrodynamic performance, cavitation, and noise of a normal skew B-series marine propeller in the cavitation tunnel. *Ocean Engineering*, vol. 238, 2021, 109739, DOI :10.1016/j.oceaneng.2021.109739.
- [12] Purwana, A., Ariana, I. M., Wardhana, W. (2021). Numerical study on the cavitation noise of marine skew propellers. *Journal of Naval Architecture and Marine Engineering*, vol. 18, no. 2, 97–107, DOI: 10.3329/jname.v18i2.38099.
- [13] Chavan, S. A., Bhattacharyya, A., Sha, O. P. (2021). Open water performance of B-Series marine propellers in tandem configurations. *Ocean Engineering*, vol. 242, 2021, 110158, DOI: 10.1016/j.oceaneng.2021.110158.
- [14] Jadmiko, E., Gurning, R. O. S., Zaman, M. B., Leksono, S., Semin, Nanda, M. I. (2019). The Effect of variation skew angle B-series propeller on performance and cavitation. *International Journal of Mechanical Engineering and Technology*, vol. 10, no. 5, 219-234.
- [15] Santosa, A.W. B., Mausulunnaji, M. F., Setiyobudi, N., Chrismianto, D., Hadi E. S. (2022). Engine propeller matching analysis on fishing vessel using inboard engine. *Journal of Applied Engineering Science*, vol. 20, no. 2, 477-485, DOI: 10.5937/jaes0-31979.
- [16] Windyandari, A., Haryadi G. D., Suharto. (2018). Design and performance analysis of B-series propeller for traditional purse seine boat in the north coastal region of central Java Indonesia. *Journal of Applied Engineering Science*, vol. 16, no. 4, 494-502, DOI:10.5937/jaes16-18506.
- [17] Yilmaz, N., Atlar, M., Khorasanchi, M. (2019). An improved mesh adaption and refinement approach to cavitation simulation (MARCS) of propellers. *Ocean Engineering*, vol. 171, 2019, 139-150, DOI:10.1016/j.oceaneng.2018.11.001.
- [18] Tu, T. N. (2019). Numerical simulation of propeller open water characteristics using the RANSE method. *Alexandria Engineering Journal*, vol. 58, no. 2, 531-537, DOI:10.1016/j.aej.2019.05.005.
- [19] Chien, N. M. (2015). Investigation of the capability of RANSE CFD for propeller calculation in practical use. Master's thesis, Université de Liège, Liège, Belgique, Matheo, from <http://hdl.handle.net/2268.2/6169>, accessed on 2015.
- [20] Lungu, A. (2019). Hydrodynamic loads and wake dynamics of a propeller working in oblique flow. *IOP Conference Series: Materials Science and Engineering 2019*, p. 012055.
- [21] Guerrero, A. M., Gonzalez-Gutierrez, L. M., Remola, A. O., Diaz-Ojeda, H. R. (2018). On the influence of transition modeling and cross-flow effects on open water propeller simulations. *Ocean Engineering*, vol. 156, 2018, 101-119, DOI: 10.1016/j.oceaneng.2018.02.068.
- [22] Eom, M. J., Jang, Y. H., Paik, K. J. (2021). A study on the propeller open water performance due to immersion depth and regular wave. *Ocean Engineering*, vol. 219, 2021, 108265, DOI:10.1016/j.oceaneng.2020.108265.
- [23] Kim, K. W., Paik, K. J., Lee, J. H., Song, S. S., Altar, M., Demirel, Y. K. (2021). A study on the efficient numerical analysis for the prediction of full-scale propeller performance using CFD. *Ocean Engineering*, vol. 240, 2021, 109931, DOI:10.1016/j.oceaneng.2021.109931.
- [24] Sánchez, A. R., Andrés, J., Rio, S. D., Quintana, E.C., Sanín-Villa, D. (2023). Numerical comparison of savonius turbine as a rotor for gravitational vortex turbine with standard rotor. *Journal of Applied Engineering Science*, vol. 21, no. 1, 204-211, DOI:10.5937/jaes0-39847.
- [25] Kamran, M., Nouri, N, M.(2021). Regression Modeling of surface piercing propeller performance based on trailing edge geometrical parameters using CFD method. *Ocean Engineering*, vol 259, September 2022, 111752, DOI. 10.1016/j.oceaneng.2022.111752

- [26] Zhai, S., Jin, S., Chen, J., Liu, Z., Song, X. (2022). CFD-based multi-objective optimization of the duct for a rim-driven thruster. *Ocean Engineering*, vol 264, November 2022, 112467, DOI. 10.1016/j.oceaneng.2022.112467.
- [27] Machfudin, A., Dinariyana, A., Purnamasari, D., (2022). Analysis of uncertainties in open water test of B-series propeller at Indonesian Hydrodynamic Laboratory. *IOP Conference Series: Earth and Environmental Science* 2022, 012022.
- [28] Delen, C., Bal, S. (2023). A comprehensive experimental investigation of total drag and wave height of ONR Tumblehome, including uncertainty analysis. *Ocean Engineering*, vol 284, September 2023, 115232, DOI. 10.1016/j.oceaneng.2023.115232.
- [29] Park, J., Lee, D., Park, G., Rhee, S, H., Seo, J., Yoon, H, K. (2022). Uncertainty assessment of outdoor free-running model tests for maneuverability analysis of a damaged surface combatant. *Ocean Engineering*, vol 252, May 2022, 111135, DOI. 10.1016/j.oceaneng.2022.111135.
- [30] Dalheim, O, O., Steen, S. (2021). Uncertainty in the real-time estimation of ship speed through water. *Ocean Engineering*, vol 235, September 2021, 109423, DOI. 10.1016/j.oceaneng.2021.109423.
- [31] Dubois, A., Leong, Z, Q., Quyen, H, D., Binns, J, R. (2019). Uncertainty estimation of a CFD-methodology for the performance analysis of a collective and cyclic pitch propeller. *Applied Ocean Research*, vol. 85, April 2019, 73-78, DOI. 10.1016/j.apor.2019.01.028.
- [32] Aram, S., Mucha, P. (2023). Computational fluid dynamics analysis of different propeller models for a ship maneuvering in calm water. *Ocean Engineering*, vol. 276, 15 May 2023, 114226, DOI. 10.1016/j.oceaneng.2023.114226.
- [33] Utama, I. K. A. P., Purnamasari, D., Suastika, I. K., Nurhadi, N., Thomas, G. A. (2021). Toward improvement of resistance testing reliability. *Journal of Engineering and Technological Sciences*, vol. 5, no.2, 210201, DOI:10.5614/j.eng.technol.sci.2021.53.2.1.
- [34] Purnamasari, D., Utama, I., Suastika, I. K., Thomas, G. (2020). Application of kalman filter to the uncertainty of model resistance data obtained from experiment. *Journal of Engineering Science and Technology*, vol. 15, no. 2, 1455-1465, from <https://discovery.ucl.ac.uk/id/eprint/10088338>.
- [35] Purnamasari, D., Utama I.K, A. P., Suastika, I. K. (2020). Verification and validation of a resistance model for tanker 17.500 dwt. *The Journal of Marine Science and Technology*, vol. 28, no. 1, from <https://jmsst.ntou.edu.tw/journal/vol128/iss1/3>.
- [36] Roache, P. J. (1998). *Verification and validation in computational science and engineering*, Hermosa Publishing, Socorro New Mexico.

Paper submitted: 24.03.2023.

Paper accepted: 18.10.2023.

This is an open access article distributed under the CC BY 4.0 terms and conditions